Characterization of $Si/Si_{1-y}C_y$ superlattices grown by surfactant assisted molecular beam epitaxy*

P. O. Pettersson,[a] C. C. Ahn, and T. C. McGill
Department of Applied Physics, California Institute of Technology, Pasadena, California 91125

E. T. Croke and A. T. Hunter
Hughes Research Laboratories, Malibu, California 90265

(Received 22 January 1996; accepted 26 April 1996)

$Si/Si_{0.97}C_{0.03}$ superlattices grown on Si(001) substrates by Sb surfactant assisted molecular beam epitaxy are characterized by *in situ* reflection high energy electron diffraction (RHEED), atomic force microscopy, transmission electron microscopy (TEM), and high resolution x-ray diffraction. The RHEED shows that, in the absence of Sb, the growth front roughens during $Si_{0.97}C_{0.03}$ growth and smooths during subsequent Si growth. In contrast, when Sb is present, the growth front remains smooth throughout the growth. This observation is confirmed by cross-sectional TEM, which reveals that for samples grown without the use of Sb, the $Si/Si_{0.97}C_{0.03}$ interfaces ($Si_{0.97}C_{0.03}$ on Si) are much more abrupt than the $Si_{0.97}C_{0.03}/Si$ interfaces. In the case of Sb assisted growth, there is no observable difference in abruptness between the two types of interfaces. Atomic force microscopy micrographs of the $Si_{0.97}C_{0.03}$ surface reveal features that could be the source of the roughness observed by RHEED and TEM.

I. INTRODUCTION

By introducing carbon into the Si/Ge material system, one could increase flexibility in the design of electronic structure in a Si-based electronics technology. The reason for this is that the SiGeC alloys may provide useful conduction band offsets for layers grown coherently strained to Si. This offset might allow fabrication of novel *n*-type devices such as *n*-type resonant tunneling devices (RTDs) or high-electron-mobility transistors (*n*-HEMTs) that are compatible with VLSI processing lines. In addition, due to the smaller lattice constant of diamond (a_0=0.357 nm vs a_0=0.543 nm for Si and a_0=0.566 nm for Ge), carbon could be used for strain compensation of SiGe structures, resulting in alloy layers that are lattice-matched to Si and therefore in devices that are stable during high temperature processing steps.

When $Si_{1-x}Ge_x$ is grown coherently strained to Si(001), the compressive strain causes the fourfold-degenerate Δ_4 band to become the lowest conduction band state. The combination of strain splitting and compositional shift cancel for this band, resulting in almost no conduction band offset for $Si_{1-x}Ge_x$ alloys grown strained to Si.[1]

While conduction band offsets can be achieved in the $Si/Si_{1-x}Ge_x$ system by growing tensile-strained layers on relaxed $Si_{1-x}Ge_x$ buffer layers, the incorporation of carbon may provide this desirable feature without the substantial defect densities and complicated processing inherent for growth on relaxed buffer layers. Since $Si_{1-x-y}Ge_xC_y$ alloys can be grown lattice matched to Si, the strain splitting of the conduction band can be eliminated and a useful conduction band offset might be provided by a compositional shift in band gap. According to estimates,[1] the band gap for $Si_{1-y}C_y$ alloys strained to Si decreases only slightly with y. Therefore, it is essential to develop growth techniques that allow the introduction of substantially more than 1% carbon to achieve band gap differences and band offsets that are larger than k_BT at room temperature.

Our experiments show that for carbon concentrations in excess of 2%, the normal, two-dimensional layer-by-layer growth of Si(100)[2] is disrupted, resulting in a rough surface. This roughness manifests itself in reflection high energy electron diffraction (RHEED) as ''spottiness'' in the pattern, rather than the normally streaked, $(2\times1)+(1\times2)$ pattern associated with growth on atomically smooth, two-domain-reconstructed Si(001) surfaces.

In this article, we report a study of surfactant-mediated growth of $Si/Si_{0.97}C_{0.03}$ superlattices through the use of RHEED, transmission electron microscopy (TEM), atomic force microscopy (AFM), and high resolution x-ray diffraction (HRXRD). The RHEED and TEM results were reported in Ref. 3; here we explain the RHEED analysis in detail and correlate the previous results with AFM measurements. Actual composition and layer thicknesses were confirmed using HRXRD. We demonstrate that through the use of a surfactant, the tendency for the $Si_{1-y}C_y$ surface to roughen during growth can be reduced or eliminated, allowing layers with even higher carbon concentrations to be grown. This technique has been used previously with encouraging results to suppress Stranski–Krastanov islanding during the growth of Si/Ge superlattices[4] and $Ge_{1-y}C_y$ alloy layers[5] on Si substrates.

The article is organized as follows. First, the sample growth is described. Details of the superlattice structure and postgrowth compositional analysis by HRXRD is presented. We then present an analysis of digitized RHEED data taken during growth of the samples and discuss the findings in

*Published without author corrections.
[a]Electronic mail: peo@ssdp.caltech.edu

comparison with cross-sectional TEM micrographs and AFM images of the sample surfaces. Finally, we put forward an explanation as to how the surfactant might suppress the islanding.

II. EXPERIMENT

The samples used in this experiment consisted of two 15-period, 26.1 nm Si/4.4 nm $Si_{0.97}C_{0.03}$ superlattices grown at 525 °C on 100-nm-thick Si buffer layers. Prior to growth 2000 Ω cm Si(001) substrates were degreased in trichloroethane and acetone for 2 min each, followed by rinses in methanol for 10 min and de-ionized H_2O. A 15 s dip in 5% HF just prior to loading into the MBE system (Perkin–Elmer Model 430S) was used to hydrogen passivate the wafer surfaces. *In situ*, the wafer surfaces were cleaned at 875 °C under the influence of a slight Si flux (about 0.1 Å/s) until the RHEED pattern consisted of the usual $(2\times1)+(1\times2)$ streaked pattern indicative of a clean, reconstructed Si(001) surface.

After deposition of a 100 nm undoped Si buffer layer, approximately one monolayer (6.8×10^{14} atoms/cm^3) of Sb was deposited on the surface of sample SL-Sb. Sample SL received no such Sb predeposition. The superlattices were then grown on each sample using growth rates of approximately 1.8 Å/s and 0.015 Å/s for Si and C, respectively, evaporated from electron beam sources. The $Si_{0.97}C_{0.03}$ layer was grown with both shutters opened, so the growth rate for this layer was 1.815 Å/s. Closed-loop control of the flux was accomplished for Si through the use of a Sentinel III deposition controller and for C by monitoring the amplitude of amu 36 (C_3) with a residual gas analyzer (RGA) and adjusting the power to the electron gun to maintain a predetermined signal. Growth rates, layer thicknesses, and compositions were determined later using HRXRD. From the superlattice peak positions, the average carbon concentration and superlattice period were measured and, together with a knowledge of the shutter opening times, used to calculate individual layer thicknesses and the carbon content of the $Si_{1-y}C_y$ layer.

During superlattice growth, images of the RHEED patterns were digitized and captured for later analysis. The setup consisted of a standard RHEED system (Perkin–Elmer), a black and white CCD camera (SONY CCD-IRIS), and an S-VHS VCR (Panasonic AG 7355). Data were recorded on S-VHS videotape and digitized at a resolution of 512×512 pixels with a 256 level grayscale using a computer (Sun Sparc 2) and a video capture board (Data Cell S2200). In order to filter out some of the background due to stray light from the e-gun sources, we inserted a green filter between the camera and the RHEED screen.

The AFM measurements were performed in laboratory ambient without any surface preparation using a Nanoscope III from Digital Instruments. The TEM cross sections were prepared by mechanical polishing and ion milling and the micrographs were acquired at an acceleration voltage of 300 kV on a Philips EM430 electron microscope.

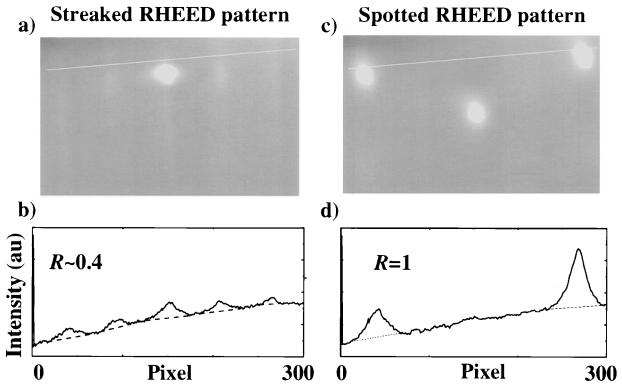

FIG. 1. Analysis of the RHEED pattern. The amplitudes of the intensity along the line [marked in white in (a) and (c)] are shown in (b) and (d). The areas enclosed by the solid curves and the dotted lines in (b) and (d) represent the total intensity associated with that streak or spot. By calculating the ratio of the spot intensity to the total intensity of the pattern, we obtain a qualitative measure of the roughness of the surface R [see Eq. (1)]. This ratio can be used as a qualitative measure of surface roughness since, for a spotty pattern (c), the areas associated with the spots will dominate, making $R\approx1$. On the other hand, when the RHEED pattern is streaked (a), all the areas are comparable, giving an R of about $\frac{2}{5}=0.4$.

III. RESULTS

The RHEED pattern from both samples prior to growth of the Si buffer layer exhibited the usual $(2\times1)+(1\times2)$ streaked pattern typical of a clean Si(001) surface. During growth of sample SL, immediately upon opening the carbon shutter, the pattern became spotty in appearance, indicative of a rough surface. Each subsequent Si layer caused the pattern to revert back to the (2×1)-reconstructed pattern, suggesting that the Si deposition caused the surface to become smooth again. This alternating behavior of roughening followed by smoothing persisted throughout the growth of this sample. For sample SL-Sb, the half-order streaks originally visible in the pattern diminished in intensity after Sb deposition due to a realignment of the surface reconstruction.[6] The observed (1×1) pattern exhibited no spottiness during the subsequent growth of the superlattice and remained streaked (smooth).

In order to study the differences between the spotted and streaked patterns observed in the growth of sample SL, we employed the following analysis of the digitized RHEED data. First, the intensity along a line [marked in white in Figs. 1(a) and 1(c)] perpendicular to the streak direction and intersecting the (10) and (10) spots was digitized. The amplitude of the intensity along the line is shown in Figs. 1(b) and 1(d). Then, the intensity associated with a certain spot or streak $(n0)$ was integrated along the line, to take into account the intensity from the full width of the streak or spot, to give the quantity I_{n0}. The background intensity due to light from the e-gun sources was subtracted, as indicated by the dotted lines in Figs. 1(b) and 1(d). Finally, we calculated the ratio, R, of the spot intensity to the intensity of the whole pattern [see Eq. (1)]. This ratio can then be used as a qualitative measure of surface roughness since, for a spotty pattern, $I_{\bar{1}0}$ and I_{10} will dominate, making $R\approx1$. On the other hand, when the RHEED pattern is streaked [see Figs. 1(a)

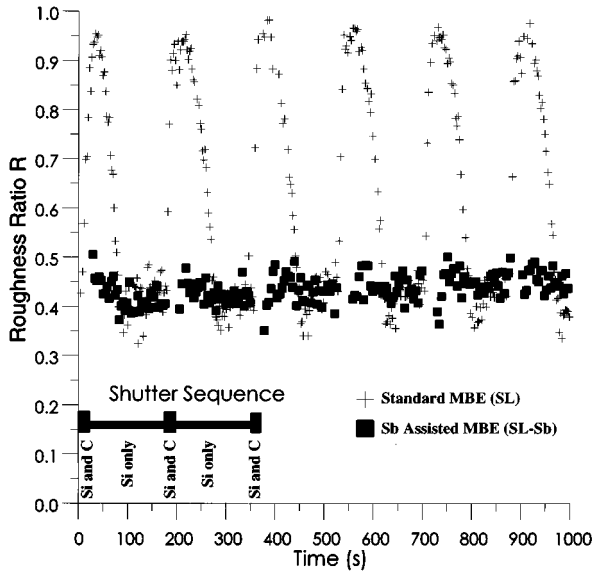

FIG. 2. Roughness ratio R vs growth time. See Fig. 1 for the derivation of R. An R of 1 indicates a spotted RHEED pattern and an R of 0.4 indicates a streaked pattern. For sample SL (no Sb predeposition), immediately upon opening the C shutter the ratio is shown to increase rapidly, saturating at a value near 1. Half ($\approx$13 nm) of the Si layer thickness was required to completely recover the original pattern. During growth of sample SL-Sb, the RHEED pattern remained unchanged from the (1×1), streaked pattern observed immediately following Sb predeposition.

and 1(b)], all the terms are of comparable magnitude, giving an R of about $\frac{2}{5}=0.4$.

$$R=\frac{I_{\bar{1}0}+I_{10}}{I_{\bar{1}0}+I_{\bar{\frac{1}{2}}0}+I_{00}+I_{\frac{1}{2}0}+I_{10}}. \quad (1)$$

In Fig. 2(d), the ratio, R, is plotted as a function of time during growth of the two samples (C shutter opens at $t=0$ s). For sample SL (no Sb predeposition), immediately upon opening the C shutter the ratio is shown to increase rapidly, saturating at a value near 1. During subsequent growth of the Si layer, the RHEED pattern slowly recovered its original (2×1)+(1×2), streaked pattern and the ratio returned to approximately 0.4 (smooth). From Fig. 2, we note that fully half ($\approx$13 nm) of the Si layer thickness was required to completely recover the original pattern. During growth of sample SL-Sb, the RHEED pattern remained unchanged from the (1×1), streaked pattern observed immediately following Sb predeposition. Data were not available for SL-Sb during $Si_{0.97}C_{0.03}$ deposition because stray light from the e-guns washed out the pattern. Nevertheless, it was possible to view the pattern visually during these periods and no spottiness was observed.

In Fig. 3, we present cross-sectional TEM images of the samples that show features consistent with the RHEED observations. Figure 3(a) is an image taken from sample SL, showing alternating thick and thin layers corresponding to the Si and $Si_{0.97}C_{0.03}$ layers, respectively. The surface of the superlattice is marked A near the top of the figure. Clearly, the interfaces that are formed when $Si_{0.97}C_{0.03}$ is grown on Si

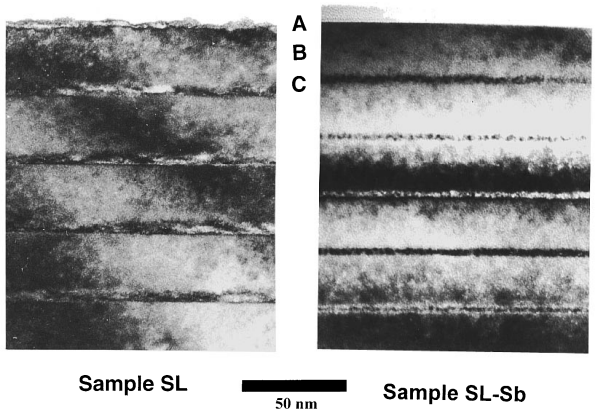

FIG. 3. Cross-sectional TEM images of the superlattice samples. (a) is an image taken from sample SL, showing alternating layers of thick and thin bands corresponding to the Si (B) and $Si_{0.97}C_{0.03}$ (C) layers, respectively. The surface of the superlattice is marked A near the top. Sample SL (a) was terminated with a $Si_{0.97}C_{0.03}$ layer resulting in rough surface morphology (see Fig. 5). Sample SL-Sb (b) was terminated with a Si layer. Clearly, the interfaces that are formed when $Si_{0.97}C_{0.03}$ is grown on Si are much more abrupt than the interfaces formed when Si is grown on $Si_{0.97}C_{0.03}$. In the case of sample SL-Sb (b), both interfaces appear equally abrupt. In comparison with sample SL, they appear more abrupt than the case for which Si is grown on $Si_{0.97}C_{0.03}$ and less abrupt than the case for which $Si_{0.97}C_{0.03}$ is grown on Si.

are much more abrupt than the interfaces formed when Si is grown on $Si_{0.97}C_{0.03}$. In the case of sample SL-Sb [Fig. 3(b)], both interfaces appear equally abrupt. In comparison with sample SL, they appear more abrupt than the case for which Si is grown on $Si_{0.97}C_{0.03}$ and less abrupt than the case for which $Si_{0.97}C_{0.03}$ is grown on Si. Sample SL was terminated with a $Si_{0.97}C_{0.03}$ layer, resulting in a rough surface morphology evident in the TEM and AFM micrographs (see Fig. 5). Sample SL-Sb was terminated with a Si layer, which gives the superlattice a smooth surface morphology.

In Fig. 4, we display HRXRD of the two samples. The peaks associated with sample SL are larger in magnitude and have narrower widths than those of sample SL-Sb. One reason for this could be that the $Si_{0.97}C_{0.03}$/Si interfaces (when $Si_{0.97}C_{0.03}$ is grown on Si) in sample SL are more abrupt than the $Si/Si_{0.97}C_{0.03}$ interfaces in sample SL-Sb, as seen in the TEM image (see Fig. 3). Another reason might be that there is a higher density of defects that look like stacking faults in sample SL-Sb as compared to sample SL. These defects could reduce the lateral coherence of the superlattices and thus broaden the HRXRD peaks. The defects are discussed in more detail below. As mentioned above, the superlattice peak positions were measured to calculate the layer thicknesses and carbon content of the samples.

In Fig. 5, we show an AFM micrograph taken from the surface of sample SL, terminated with $Si_{0.97}C_{0.03}$. The figure shows features on the order of 1.5 nm peak-to-valley perpendicular to the surface and 40.0 nm laterally. There does not appear to be any directional dependence to the features. The RMS roughness of this surface was measured to be approximately 0.36 nm. These features are apparently responsible for the spotted pattern observed in the RHEED image of Fig. 1(c), since additional samples we have studied, for which Si

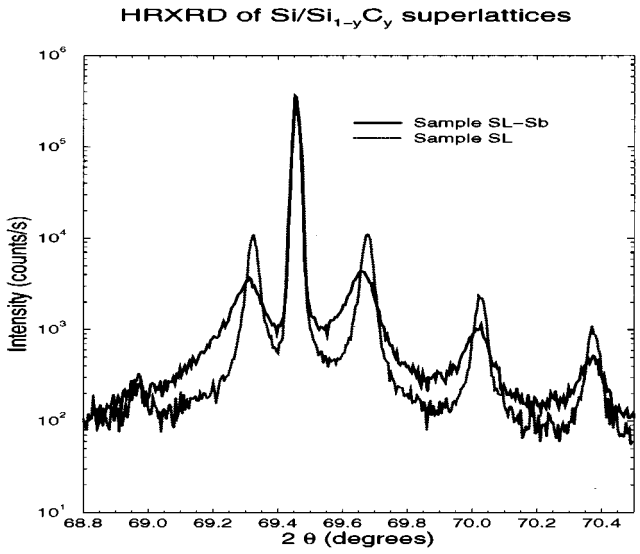

FIG. 4. HRXRD of a 15 period $Si/Si_{0.97}C_{0.03}$ superlattice grown by standard MBE (sample SL) and by Sb assisted MBE (sample SL-Sb). The sample SL superlattice peaks are sharper than those of sample SL-Sb. This is probably due to the $Si/Si_{0.97}C_{0.03}$ interfaces being less sharp in the SL-Sb sample (as observed in the cross-sectional TEM micrographs, Fig. 3) or a higher density of stacking faults in sample SL-Sb as compared to sample SL.

in one sample and Sb-terminated $Si_{0.985}C_{0.015}$ in another were grown on Si(001), lack these features and have streaked RHEED patterns. The feature height observed in the AFM micrograph agrees with the thickness variation seen in the TEM image [see Fig. 3(a)].

In addition to the interface structure, the TEM images also reveal that here are defects that look like stacking faults, possibly originating from point defects such as C dimers or trimers in the SL-Sb sample. These defects are also present in the SL sample, albeit at a lower density. Most of the defects in sample SL-Sb originate in the region between superlattice layers 7 and 10 (counting up from the bufferlayer). Only a small fraction (0.4%) of the volume of the superlattice is enclosed by these defects.

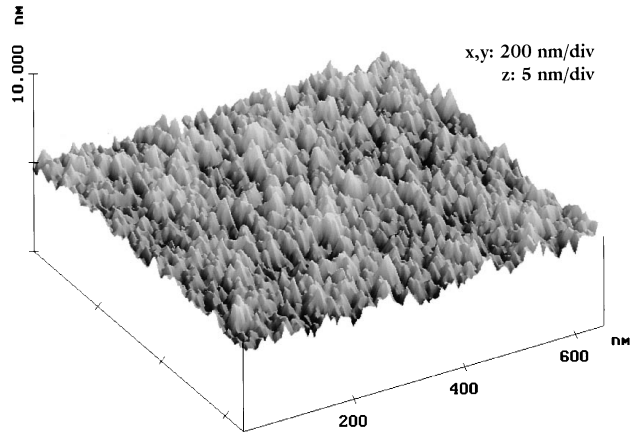

FIG. 5. AFM micrograph of the top layer ($Si_{0.97}C_{0.03}$) of a 15 period $Si/Si_{0.97}C_{0.03}$ superlattice grown by standard MBE (sample SL). The features are on the order of 1.4 nm tall and 40 nm on the side. These surface features apparantly give rise to the spotty RHEED pattern observed [see Fig. 1(c)] and the variation in thickness seen in the TEM (see Fig. 3).

IV. DISCUSSION

The data presented in the above section suggest that one or more of the species in the carbon flux disrupts the epitaxial growth of $Si_{0.97}C_{0.03}$ on Si (sample SL). These species form surface nucleation centers where diffusing adatoms can incorporate in competition with surface steps, resulting in 3D growth. Residual gas analysis of the growth flux shows that it primarily consists of monomers (C), dimers (C_2), and trimers (C_3). In principle, any of the carbon species could act as nucleation centers. We expect the monomers to be the most mobile on the surface, and hence, the most likely to simply be incorporated in step flow growth. Of multiple carbon species the dominant is the dimers.

All of the multiple carbon species, however, are potential candidates for nucleating the rough growth. First, the C–C bond is 1.8 times stronger than the Si–Si bond and based on the observation that the Si dimer is stable up to 600 K,[8] one expects the C dimer and trimers to be stable up to 1100 K or about 800 °C. Since the growth temperature used in this experiment was 525 °C, the carbon dimers and trimers impinging on the surface remain undissociated. Another argument for the stability of the carbon dimers is that the equilibrium constant for sublimation of solid carbon (to monoatomic carbon gas), K_p, is 3×10^{-17} at the growth temperature mentioned above.

Second, the diffusion length of these dimers and trimers is expected to be negligible compared to that of the monomers because of the large activation energy due to the bond bending and stretching required for a dimer or trimer to move on the surface. Thus, while the monomers might diffuse to a step and thus contribute to step flow growth, the dimers or trimers will incorporate at the site of impingement and form nucleation centers.

Third, the nucleation center density generated by the dimers and trimers is large enough for 3D growth to dominate over 2D step flow growth. To show one possibility for how this could occur, we need to consider this probability of an adatom attaching to a dimer or trimer rather than to a step. To assess the relative probability, we follow Mo *et al.*'s argument.[8] Adapting his argument, we consider a square with the side aligned with a step on a slightly miscut substrate. We set the length of the side equal to the average terrace width W of the steps which is given by the degree of miscut of the substrate. Under the conditions of our experiment, this square is the area from which this portion of the step accumulates adatoms. Let us say that the square has a dimer at the center and assume that both the step and the dimer are perfect sinks for adatoms. According to the 2D random walk theory, the number of hops required for an adatom impinging at a random site in the square to reach the dimer is on average $\sim(W/a)^2$, where a is the length of a hop. The number of hops required for the adatom find the step is also on average $\sim(W/a)^2$. In this case then, both island growth and step flow

growth will take place. For both sample SL and SL-Sb, the fluxes of the dimers and trimers were about 10% and 5% of the monomer flux, respectively. These fluxes yield a dimer and trimer density of about 10^{12} molecules/cm^2 in the time required to complete a monolayer of $Si_{0.97}C_{0.03}$ growth. Given a limiting case of a wafer miscut of about 0.5°, the terrace width is $W \approx 2\times10^{-6}$ cm. At the density calculated above, we get four dimers per square, so 3D nucleation should compete effectively with 2D step-flow growth.

We speculate that in the case of sample SL-Sb, where the surface stays smooth throughout the growth, the surfactant assisted growth mechanism prevents the dimers and trimers from forming effective nucleation centers. The primary role of the Sb is to ride as a surface layer, burying the carbon dimer and trimers. An impinging silicon adatom diffuses on the Sb layer until it reaches a proper site. At that site, the adatom undergoes an exchange with a surfactant atom and incorporates. Again, the carbon clusters do not diffuse on the surface; rather, they are incorporated immediately by some exchange mechanism. Since direct contact between Si adatoms and the carbon clusters is reduced, the clusters no longer serve as effective nucleation centers and the growth stays relatively smooth as shown by AFM and the streaked RHEED pattern.

The TEM picture in Fig. 3 shows that the interface between the Si and $Si_{0.97}C_{0.03}$ on the substrate side is slightly rougher on a sample superlattice grown with Sb than it is on a sample grown without Sb. One possible reason for this is that, in our case, a perfectly ordered Sb terminated Si(001) surface was not achieved [RHEED pattern was (1×1) as opposed to (2×1)]. The unordered surface could prompt the exchange to occur at sites other than steps, thus creating a less abrupt growth front. A highly ordered Sb-terminated (2×1)-reconstructed surface could be expected to aid in the formation of perfectly flat interfaces.

In conclusion, the Sb prevents the carbon dimers and trimers from serving as effective nucleation centers for 3D growth and as a consequence the surface stays smooth during growth of $Si_{0.97}C_{0.03}$ on a sample grown with Sb (sample SL-Sb), whereas the surface roughens during $Si_{0.97}C_{0.03}$ growth on the sample grown without Sb (sample SL).

V. SUMMARY

We studied the effect of adding Sb as a surfactant in the MBE growth of $Si/Si_{0.97}C_{0.03}$ superlattices. Our analysis of reflection high energy electron diffraction, transmission electron microscopy, x-ray diffraction, and atomic force microscopy data shows that Sb induces 2D growth of $Si_{0.97}C_{0.03}$ under conditions in which standard MBE yields 3D growth. Epitaxial growth on the 2×1 Si(001) surface could be easily disrupted by carbon dimers and trimers which introduce additional sites for incorporation of Si adatoms. The Sb-terminated Si surface could prevent direct contact between the carbon dimers and the silicon, and hence suppresses the tendency of the surface to roughen. In conclusion, the use of Sb as a surfactant during growth of high-carbon-content $Si_{0.97}C_{0.03}$ alloys was shown to result in sharper film interfaces and appears useful for achieving carbon contents in excess of what would normally be possible for growth on bare Si(001).

ACKNOWLEDGMENTS

This study was supported in part by the Office of Naval Research under Grant No. N00014-93-1-0710. In addition, the authors would like to thank Carol Garland for her assistance in obtaining the TEM images presented in this work.

[1]A. R. Powell, K. Eberl, F. K. LeGoues, B. A. Ek, and S. S. Iyer, J. Vac. Sci. Technol. B **11**, 1064 (1993).
[2]Y.-W. Mo, R. Kariotis, D. E. Savage, and M. G. Lagally, Surf. Sci. **219**, L551 (1989).
[3]P. O. Pettersson, C. C. Ahn, T. C. McGill, E. T. Croke, and A. T. Hunter, Appl. Phys. Lett. **67**, 2530 (1995).
[4]K. Fujita, S. Fukatsu, H. Taguchi, T. Igarashi, Y. Shiraki, and R. Ito, Mater. Res. Soc. Proc. **220**, 193 (1991).
[5]H. J. Osten, E. Bugiel, and P. Zaumsel, J. Cryst. Growth **142**, 322 (1994).
[6]J. Nogami, A. A. Baski, and C. F. Quate, Appl. Phys. Lett. **58**, 475 (1991).
[7]Y. W. Mo and M. G. Lagally, Surf. Sci. **248**, 313 (1991).
[8]Y. W. Mo, J. Kleiner, M. B. Webb, and M. G. Lagally, Surf. Sci. **268**, 275 (1992).